Journal of Polymers and the Environment (2023) 31:698–708
https://doi.org/10.1007/s10924-022-02583-2

ORIGINAL PAPER

Biodegradation of Composites of Polylactic Acid and Microfibrillated Lignocellulose

Ferhat Yetiş[1] · Xuqing Liu[1] · William W. Sampson[1] · R. Hugh Gong[1]

Accepted: 5 September 2022 / Published online: 3 November 2022

Abstract We present a study of the controlled biodegradation of polylactic acid (PLA) reinforced with high lignin containing microfibrillated cellulose (MFLC) isolated from chemi-thermomechanical pulp. The surface of MFLC was modified using an acetylation method to decrease its polarity. Biocomposites with different MFLC and acetylated MFLC (Ac-MFLC) contents were fabricated via a solvent casting method. The biodegradation of biocomposites was performed by burying in soil and holding at 45 °C for 30 days. After soil burial, MFLC/biocomposites exhibited higher weight loss (5.4 %) compared to neat PLA (4.2 %) and Ac-MFLC/biocomposites (4.6 %). Morphological analysis results showed surface erosion of the PLA to change with the addition MFLC and Ac-MFLC, resulting in porous formations on the surface of biocomposites. These formations led to the loosening of microfibril-PLA interface in the internal structure, resulting in a significant decrease in the storage modulus of biocomposites. The biocomposites exhibited no antimicrobial properties, confirming their biotic degradability.

Graphical Abstract

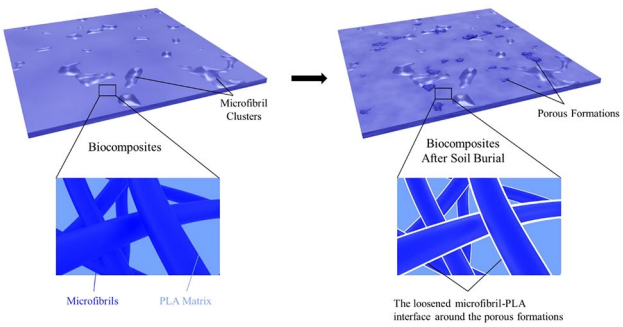

Keywords Polylactic acid · Biocomposites · Microfibrillated lignocellulose · Soil biodegradation · Viscoelastic properties

Introduction

Plastic pollution arising from petroleum-based non-biodegradable polymeric materials presents one of the great challenges of environmental management [1, 2]. Accordingly, biodegradable polymers have gained attention for replacing petroleum-based polymers. Polylactic acid (PLA) is a commercial biodegradable thermoplastic polymer derived from renewable natural sources, such as starch rich crops [3]. It has been commercialised for applications in, for example, biomedical implants [4], packaging films [5] and textile fibres [6] due to its good processability, biocompatibility,

✉ R. Hugh Gong
hugh.gong@manchester.ac.uk

Ferhat Yetiş
ferhatyetis@ogm.gov.tr

Xuqing Liu
xuqing.liu@manchester.ac.uk

William W. Sampson
william.sampson@manchester.ac.uk

[1] Department of Materials, University of Manchester, Oxford Road, M13 9PL Manchester, UK

high transparency and good mechanical performance [7]. However, its low crystallization rate, thermal stability and barrier properties need to be addressed to improve its durability and widen its application. Blending of natural nanofibres and their derivatives with PLA is a promising approach to overcome these drawbacks without compromising biodegradability [5].

Microfibrillated cellulose (MFC) consists of nanofibrillated cellulose with some micron-scale residual fibrils isolated via mechanical defibrillation of wood or plant fibres pulp. MFC has great potential for the fabrication of PLA based biocomposites due to its biodegradability, sustainability, non-toxicity and high mechanical performance [8]. Its large specific surface area, high aspect ratio and flexible fibril structure lead to interactions between adjacent fibrils, forming percolated networks which impart high strength to composites [9]. Particularly, solvent casting processing technique improve the mechanical performance of MFC-PLA biocomposites because slow solvent evaporation allows for the rearrangement of microfibrils, promoting the formation of a strong percolating network [10].

High lignin containing MFC (MFLC) is a lower-cost alternative to MFC, which is isolated from highly purified lignin-free bleached cellulosic pulp fibres. MFLC has attracted attention as it offers the advantages of high yield, low production cost and low environmental impact [11]. MFLC can be isolated from wood fibres [12–15], plant fibres [16–18] and commercial unbleached Kraft [19] and mechanical pulp fibres [20–22] without or with partial delignification process. However, the polar nature of MFLC causes fibril aggregations in non-polar polymers, resulting in a significant decrease in the mechanical performance of final composites. This can be overcome through modification of the surface of MFLC to decrease its polarity. We have shown that such surface modification using acetylation improves the dispersibility of MFLC in a PLA matrix, and hence improve the mechanical performance and thermal properties of the composite [23]. The work we describe here considers the same family of PLA-MFLC composites.

The biodegradation of PLA occurs by a two-step mechanism. The first step is abiotic hydrolysis in presence of water at high temperature, which leads to a reduction in molecular weight as the result of non-enzymatic polymer chain scission of ester groups in PLA [24]. The second step is biotic degradation in which microorganisms decompose the polymer to the biomass and CO_2 under aerobic conditions when the molecular weight of PLA reaches about 10000 to 20000 g mol^{-1} [25].

Addition of fibres or fillers in PLA can cause a change in its biodegradation behaviours. An important factor affecting the biodegradability of PLA based composites is the polar nature of the fibres, since hydroxyl groups in the structure of fibres increase the polarity of composites, leading to the acceleration of water diffusion through the weak fibre-PLA interface and consequently abiotic hydrolysis [26]. Because natural fibres are widely modified to improve the interface between fibres and PLA matrix, understanding the biodegradation behaviour of the modified fibre and PLA composite is important to developing sustainable PLA based biocomposites.

In this study, we fabricated MFLC and acetylated MFLC (Ac-MFLC) reinforced PLA biocomposites using a solvent casting method. The role of acetylation of MFLC on the biodegradation behaviours of MFLC-PLA biocomposites was investigated by determining the changes in weight loss, morphology and viscoelastic properties during the controlled soil burial.

Experimental Section

Materials

PLA (Ingeo™ Biopolymer 4043D) with a density of 1.24 g cm^{-3} and an average molecular weight of 1.3×10^5 g mol^{-1} was supplied by NatureWorks LLC (USA). Chemi-thermo-mechanical pulp (CTMP) was supplied by SCA (Sweden). Acetic anhydride and dimethylformamide (DMF) were purchased from Acros Organics (UK). Anhydrous potassium carbonate, chloroform, acetone and ethanol were purchased from Fischer Scientific (UK). Commercial topsoil was purchased from Westland (UK). All chemicals were reagent grade and used without any further purification.

Biocomposites Fabrication

Fabrication of biocomposite films is described fully in a previously published procedure [23], so here we provide a summary only. MFLC was isolated from CTMP fibres using a two-step mechanical treatment, namely high intensity laboratory beating (Medway Beater – Reed Paper, UK) for 30 min, followed by screening and homogenisation (IKA T-18) at 20000 rpm for 60 min. The chemical constitution of CTMP is provided in [23].

The acetylation of MFLC was performed with continuous stirring in a three-necked round bottomed flask equipped with reflux under N_2 flow. Freeze-dried MFLC (2 g) in DMF (100 ml) was homogenized for 2 min, and transferred to the reaction flask containing acetic anhydride (6 ml) and K_2CO_3 (0.3 g). The suspension was held at 90 °C for 1 h. After terminating the reaction by adding de-ionized water and removing the excess chemicals using centrifugation, the solution was rinsed first with deionized water at 60

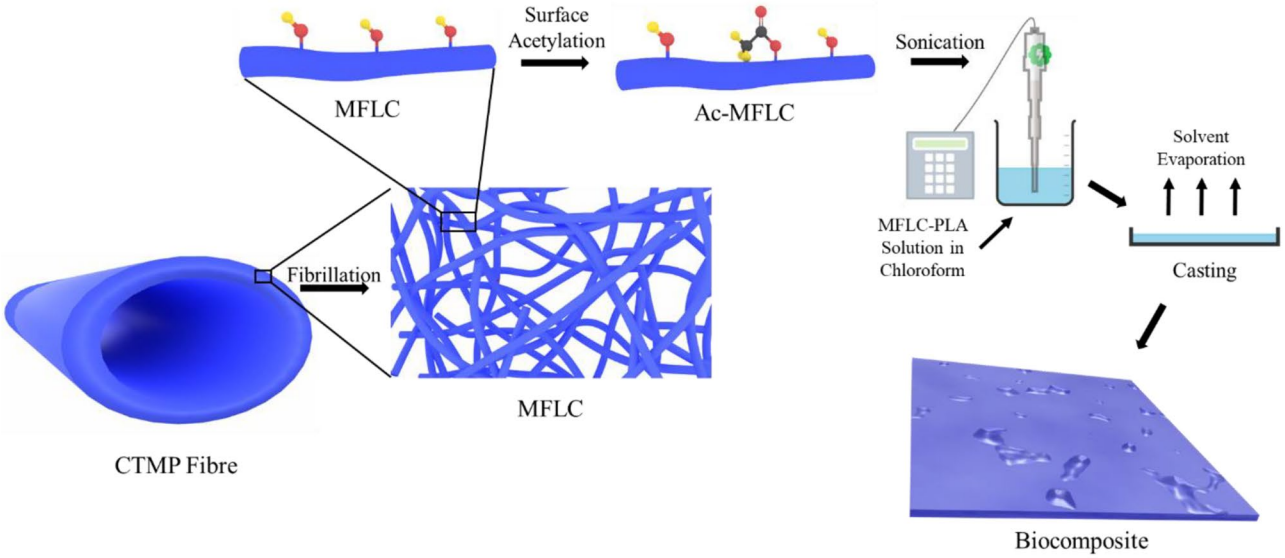

Fig. 1 Biocomposite fabrication process

°C for 2 h, and then acetone/ethanol (1:1) mixture (200 ml) at 60 °C for 2 h.

Biocomposites were fabricated using a solvent casting method. Figure 1 shows the processing route of biocomposite fabrication. PLA granules were mixed with chloroform ($CHCl_3$) until fully dissolved. The desired amount of freeze-dried MFLC or acetylated MFLC (Ac-MFLC) in $CHCl_3$ was sonicated for 2 min (QSonica – USA), and added into the dissolved PLA suspension. The final suspension was mixed under magnetic stirring for 4 h, sonicated for 2 min, and finally poured into Petri dishes for solvent evaporation at room temperature overnight. The biocomposites were dried in a vacuum oven at 40 °C for 48 h to remove any residual $CHCl_3$. Mechanical characterisation of this family of composites is provided in [23].

Soil Burial of Biocomposites

PLA and biocomposite films (20 × 20 × 0.05 mm) were sterilized with 70 % (v/v) ethanol solution followed by drying in vacuum oven at 45 °C for 24 h before the soil burial. Then, they were buried in commercial topsoil (Westland, UK) at 3–4 cm depth in perforated plastic boxes allowing aerobic conditions, and incubated at 45 °C for 30 days. The moisture content of soil was 40 %. The water loss of soil through evaporation was determined gravimetrically twice a week, and rewet to 40 % moisture content by adding distilled water. After a month in the incubator, samples were removed from the soil, washed with distilled water and 70 % (v/v) ethanol solution, and dried in vacuum oven at 45 °C for 24 h. The weight loss of the samples was calculated using Eq. 1 [27];

$$W_{loss}(\%) = \frac{W_0 - W_1}{W_0} \times 100 \quad (1)$$

where; W_0 is the weight of the dried samples before soil burial, W_1 is the weight of the samples after soil burial.

Dynamic Mechanical Analysis

The viscoelastic behaviour of biocomposite films was determined using a dynamic mechanical analyser (DMA Q800, TA Instruments) before and after soil burial. DMA was performed in tension mode under N_2 atmosphere. Rectangular biocomposite films (30 mm × 6 mm × 0.05 mm) were analysed in the temperature range 0 to 130 °C at a heating rate of 3 °C min^{-1} at a frequency of 1 Hz. The amplitude of oscillation was 15 µm.

Antimicrobial Testing

The antimicrobial tests of PLA and biocomposites were performed using the standard disk diffusion method [28]. In this test, *E. coli* and *S. aureus* were used as model Gram-positive and Gram-negative bacteria, respectively. Nutrient agar medium was prepared using Mannitol salt agar (Sigma Aldrich, UK). The agar suspension was then poured into Petri dishes, and left to completely solidify at room temperature.

The bacteria were grown in Mueller-Hinton broth (Sigma Aldrich, UK) suspension for 24 h at 37 °C, and then the suspension concentration was adjusted to 0.5 McFarland standard using mass spectrophotometry at 600 nm, which is equivalent to approximately 1.5×10^8 colony forming units

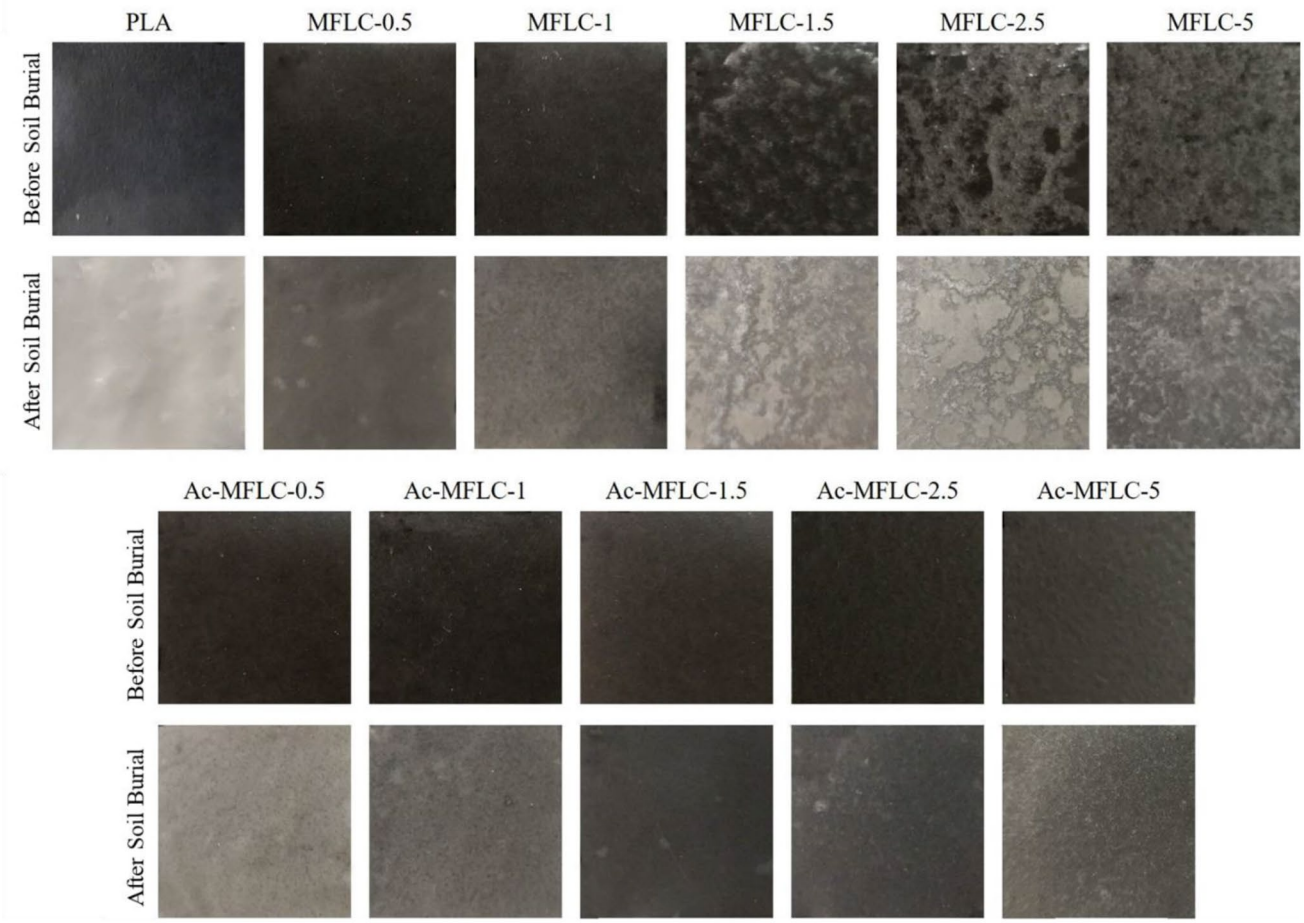

Fig. 2 Physical appearance of PLA and biocomposites before and after soil burial. The dimensions of each samples are 20 × 20 mm

(CFU ml^{-1}). The final suspension containing bacteria was spread on the solidified agar surface. PLA and biocomposite film discs (5.5 mm diameter) were placed onto bacteria inoculated agar plates. Four sample discs were placed on each agar plate and incubated for 24 h at 37 °C. After 24 h of incubation, bacterial growth on PLA and biocomposite films was recorded.

Results and Discussion

Physical Changes of Biocomposites

The influence of soil burial on the physical appearance of PLA and biocomposite films is shown in Fig. 2. The digital photo of samples was taken against a standard background using a Leica Summilux-H lens. Compared to transparent neat PLA film, all biocomposite films showed translucent structure. Increasing MFLC and Ac-MFLC contents increased the opacity of biocomposites. MFLC/biocomposites (above 1 %) exhibited extensive visible white and fluffy aggregations through the films, which is consistent with poor compatibility between MFLC and PLA. However, the Ac-MFLC/biocomposites showed no observable aggregation, indicating that surface acetylation significantly improved the dispersibility of MFLC in PLA matrix. We observed that drying samples to determine their dry weight before soil burial did not change the physical appearance of PLA and biocomposites. After the soil burial, all samples became white and opaque. This could be the result of changes in the refractive index due to the water absorption during soil burial and/or the formation of low molecular weight compounds, resulted from the hydrolytic degradation of PLA matrix [29–33]. It is clear that biocomposites with high Ac-MFLC content (above 1.5 %) were more translucent than those of MFLC/biocomposites due to the uniform dispersion of Ac-MFLC. The white and fluffy MFLC aggregations were visible through the MFLC/biocomposites after soil burial. Neat PLA and biocomposites maintained their structural integrities and exhibited no formation of any observable hole or crack, which indicates a

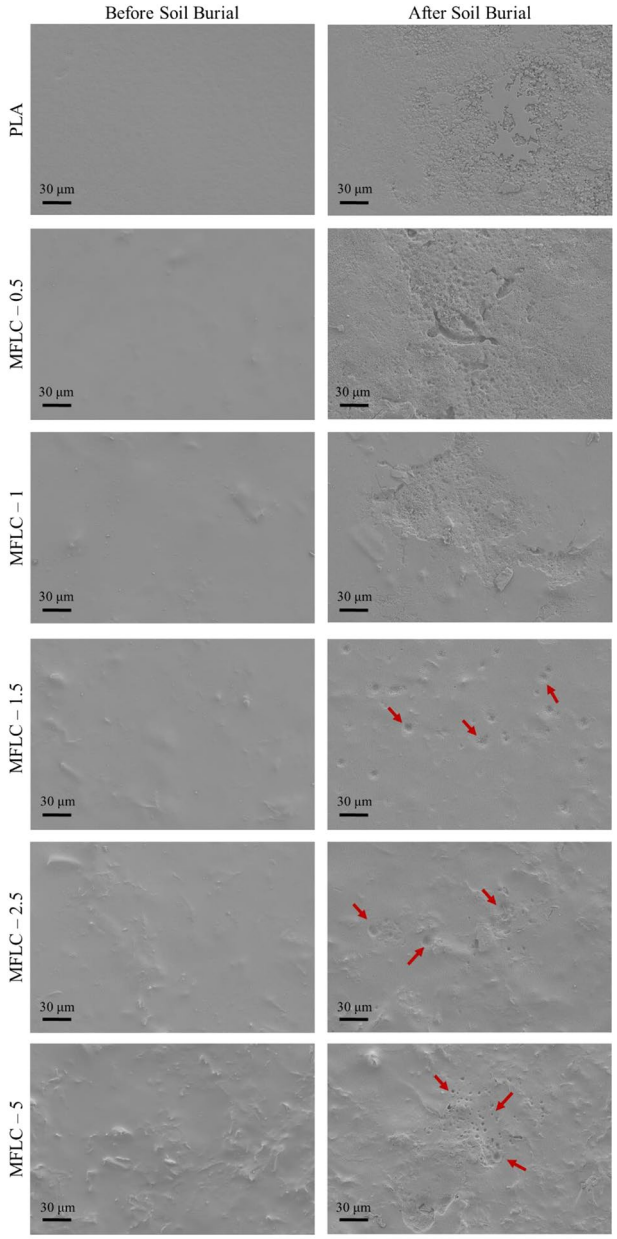

Fig. 3 SEM images of the surface morphology of PLA and MFLC/biocomposites before and after soil burial

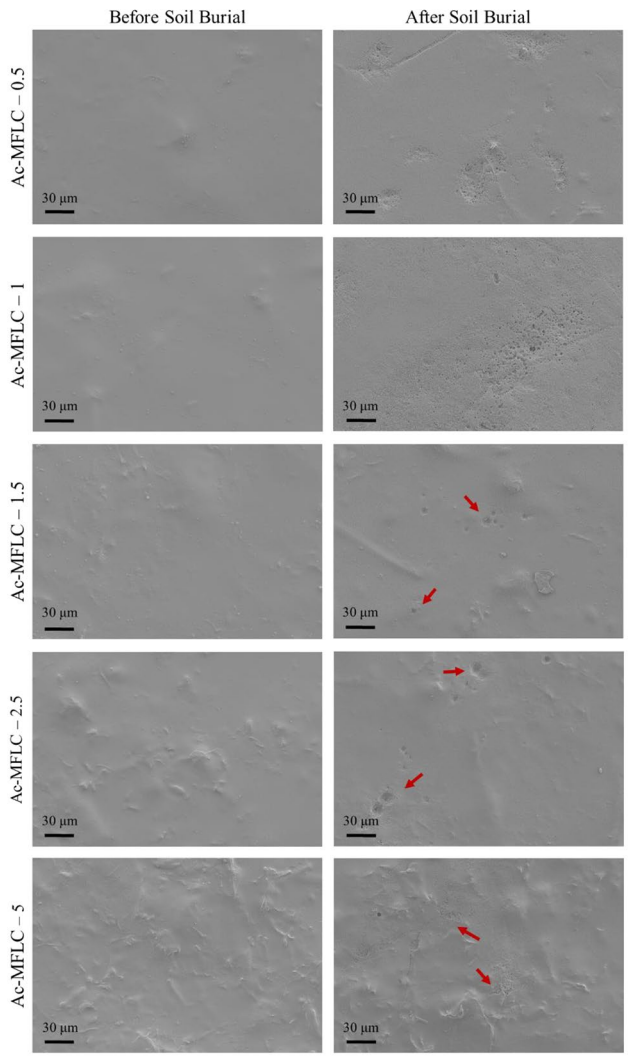

Fig. 4 SEM images of the surface morphology of Ac-MFLC/biocomposites before and after soil burial

slow degradation process of the materials under the testing conditions.

Morphological Changes of Biocomposites

The change in the surface morphologies of PLA and biocomposites after soil burial was observed using SEM to determine the effect of biodegradation. Figures 3 and 4 show the SEM images of PLA and biocomposites before and after soil burial. Low magnification images can be seen in Fig. 1 S and Fig. 2 S. Neat PLA exhibited smooth surface morphology, and no void structure was observed before the degradation. However, all biocomposites showed rough surface due to the microfibril network. The microfibril clusters were more visible at high microfibril concentrations. After soil burial, clear surface erosion appeared on neat PLA without any visible crack and hole formations, indicating that the hydrolysis of low molecular weight PLA occurred on the surface of film. Further, high incubation temperature (45 °C) increases the chain mobility facilitating the surface erosion in PLA. However, the addition of MFLC and Ac-MFLC significantly influenced the degradation behaviour of PLA. Biocomposites exhibited more localised surface erosion than PLA, which could imply that their degradation mostly occurs in regions with lower local microfibrils volume fraction. The surface of MFLC-0.5 biocomposites exhibited small channels, which are likely to be crack initiations facilitating the diffusion of water molecules and

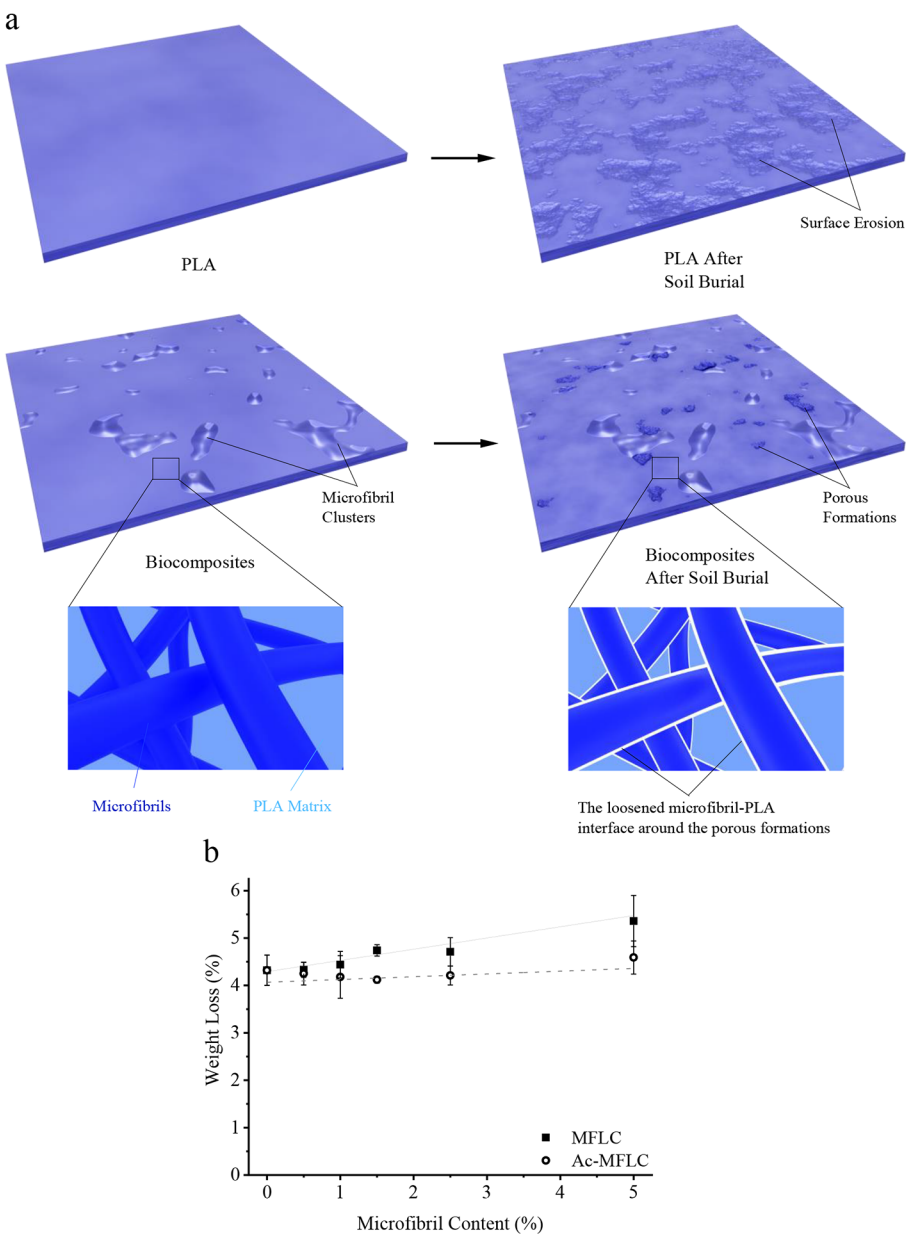

Fig. 5 Schematic illustration of the degradation characteristic of PLA and biocomposites (a). Weight loss of soil buried PLA and biocomposites (b)

microorganism through the biocomposites [34]; similar channels and cracks were reported in previous studies [35, 36]. Micron-scale porous formations were observed at the surface of biocomposites with high MFLC and Ac-MFLC contents. The porous formations are marked by red arrows in Figs. 3 and 4, and they are illustrated with a schematic diagram in Fig. 5a. It is likely that these porous formations were the pathway to the internal structure of biocomposites, and they increase the rate of water diffusion and promote the polymer hydrolysis at the inner part of biocomposites [37]. In this case, the insignificant morphologic change on the surface of biocomposites after soil burial indicates bulk degradation, which is the degradation of inner core of biocomposites as the result of faster water diffusion effect rather than hydrolytic chain scission in PLA [38]. This suggest that water penetration might be increased by microfibrils which absorbed the water molecules via hydroxyl groups in MFLC/biocomposites. In addition, the poor dispersion of MFLC into PLA leads to the formation of aggregates resulting in more water absorption, which could promote the hydrolysis of PLA. Further, absorbed water by microfibrils around the porous formations creates a moist environment at the microfibril-PLA interface, leading to polymer hydrolysis and loosening the interface [39]. This loosening effect can cause a channel formation between microfibril and PLA matrix at the internal structure of MFLC/biocomposites

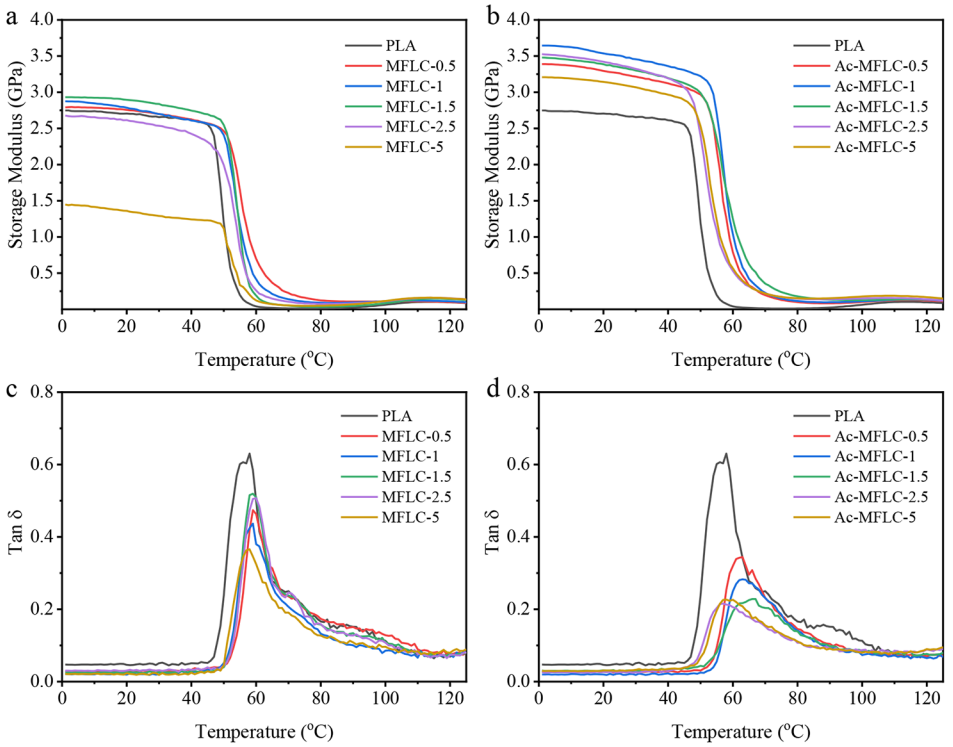

Fig. 6 Storage modulus before soil burial of MFLC/biocomposites (a), and Ac-MFLC/biocomposites (b). Tan δ before soil burial of MFLC/biocomposites (c), and Ac-MFLC/biocomposites (d)

which have a poor interface due to the polar nature of MFLC. In Ac-MFLC/biocomposites; however, the loosening effect could be lower due to the strong interface between Ac-MFLC and PLA as the result of surface acetylation. Further, the uniform dispersion of Ac-MFLC may increase the barrier properties of PLA, which could decrease the water penetration through the biocomposites.

Weight Loss of Biocomposites

The degradation rate of PLA and biocomposite films was determined by weight loss calculation (Fig. 5b). The weight loss of neat PLA was around 4.2 % after soil burial, indicating a slow degradation rate. MFLC/biocomposites exhibited slightly higher weight losses than neat PLA. Further, the weight loss increased with increasing MFLC content. This acceleration trend in the degradation rate of PLA could be due to the polar structure of MFLC which increases water absorption, promoting hydrolytic degradation at the MFLC-PLA interface where water molecules and microorganisms can diffuse into the composite materials [40]. However, the addition of Ac-MFLC did not significantly influence the weight loss of PLA. This could suggest that limited water penetration took place through the Ac-MFLC/biocomposites compared to MFLC/biocomposites, resulting in a low PLA hydrolysis at the inner core of Ac-MFLC/biocomposites.

Viscoelastic Properties of Biocomposites

The effect of MFLC and Ac-MFLC on the viscoelastic properties of PLA was determined using DMA testing. Storage modulus (*E'*) as functions of temperature for PLA and biocomposites are shown in Fig. 6a-b. Neat PLA exhibited typical semi-crystalline thermoplastic behaviour, high *E'* was observed in glassy region (<47 °C) after which it decreased sharply due to relaxation in amorphous sections of PLA in glass transition region. The addition of MFLC slightly increased the *E'* of PLA in glassy region; however, 5 % MFLC-containing biocomposite displayed a considerably low *E'* compared to PLA and other biocomposites. This might be due to microfibril aggregations resulting in a weaker interface between MFLC and PLA. On the other hand, the addition of Ac-MFLC led to a significant increase in *E'*, which may be due to the reinforcing effect of Ac-MFLC [41]. This can be attributed to the uniform dispersion of Ac-MFLC in PLA, and good stress-transfer at the interface with PLA [42]. In the glass transition region, both MFLC and Ac-MFLC biocomposites exhibited higher *E'* than neat polymer. Further, the onset drop point of *E'* shifted to a higher temperature with the addition of MFLC and Ac-MFLC. This indicates that the microfibril network protected the structural integrity of PLA [43–45]. Figure 6c-d show the plots of tan δ for PLA and biocomposites, indicating chain relaxation and microfibril-PLA interactions [46]. The intensity of tan δ for PLA decreased with the addition of

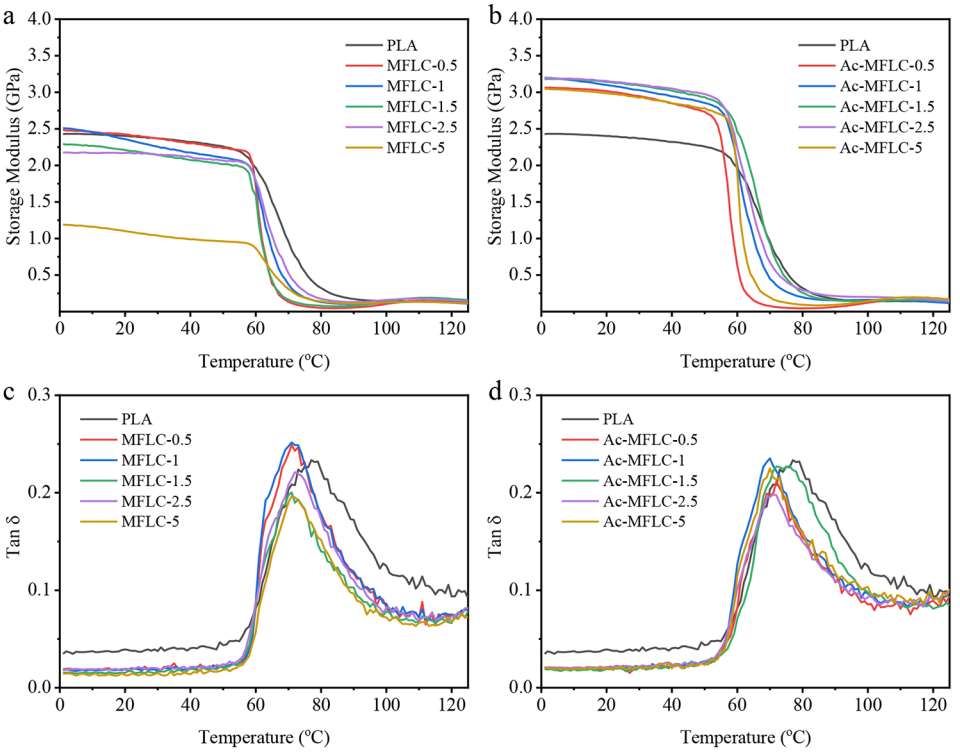

Fig. 7 Storage modulus after soil burial of MFLC/biocomposites (a), and Ac-MFLC/biocomposites (b). Tan δ after soil burial of MFLC/biocomposites (c), and Ac-MFLC/biocomposites (d)

MFLC. Further, the location of tan δ maximum for MFLC/biocomposites was 1 to 2 °C higher than for neat PLA. However, the peak shifting and decrease in the peak intensities were more visible in Ac-MFLC/biocomposites. These indicate the restriction of segmental mobility of PLA matrix with the addition of Ac-MFLC [47].

The effect of soil burial on the viscoelastic properties of PLA and biocomposites is shown in Fig. 7. It is clear that soil burial led to decreases in *E'* of PLA and biocomposites. *E'* of PLA at 30 °C decreased by around 10 % after soil burial, which might be due to surface erosion resulting from polymer hydrolysis. The decrease in *E'* for Ac-MFLC/biocomposites at the same temperature was lower than for neat PLA (Fig. 7a-b). In particular, high Ac-MFLC containing biocomposites exhibited the lowest *E'* decrease of between 4 and 6 %. This may indicate that limited loosening occurred at the interface between Ac-MFLC and PLA. Further, the uniform dispersion of Ac-MFLC in PLA matrix could decrease the water penetration, resulting in a low decrease in *E'* for biocomposites after soil burial [48]. However, the decrease in *E'* for MFLC/biocomposites at 30 °C ranged from 12 to 25 %, which were considerably higher than for Ac-MFLC/biocomposites. This can be attributed to the fact that MFLC-PLA interface loosened significantly during the soil degradation due to the polar nature of MFLC which leads to increased the water penetration, hydrolysing the polymer matrix at the interface. In glass transition region, the decrease in *E'* for PLA and biocomposites occurred gradually, which could be attributed to the annealing effect of the incubation temperature at 45 °C during degradation. This leads to the increase in the crystallinity of PLA, restricting segmental mobility in polymer chain [49, 50]. The changes of tan δ for PLA and biocomposites after soil burial are shown in Fig. 7c-d. The peak location of tan δ maximum shifted to a higher temperature and the peak intensity decreased considerably in PLA and biocomposites, indicating decreased chain mobility of polymer matrix due to increased polymer crystallinity as the amorphous phase of PLA hydrolysed during the soil burial [51]. It shows that the biodegradation under soil conditions significantly affects the viscoelastic properties of PLA and its biocomposites. Similar viscoelastic changes were reported in the literature for PLA and its blends, buried at outdoor conditions in which the soil temperature increases via sunlight, and hence increases the crystallinity of PLA [52, 53].

Antimicrobial Properties of Biocomposites

The antimicrobial activities of PLA and biocomposites were qualitatively investigated against specific Gram-negative (*E. coli*) and Gram-positive (*S. aureus*) bacteria using the disk diffusion method. Figure 3 S shows the photographs of PLA and biocomposites taken after antimicrobial testing. PLA and biocomposites exhibited no visible exhibition zone against both *E. coli* and *S. aureus*, indicating no antimicrobial activities for all samples and bacterial colonies can

grow freely around the samples. As expected, MFLC and Ac-MFLC showed no effect on the antimicrobial properties of PLA due to the bacterial degradability of the lignocellulosic constituents in the chemical structure of MFLC [54, 55]. Although acetylation increases the resistance of lignocellulosic sources against microbial attack, these sources exhibit no antimicrobial properties [56]. Therefore, acetylation did not change the antimicrobial properties of MFLC. The results showed that PLA and its biocomposites are suitable material for colonization of microbial organisms which convert the low molecular weight polymer to the monomer mass at the last stage of biodegradation under biotic soil condition.

Conclusion

We have presented an investigation into the soil biodegradation of PLA based MFLC and Ac-MFLC biocomposites fabricated using a solvent casting method. After soil burial for 30 days, the addition of MFLC slightly increased the weight loss of PLA, whereas Ac-MFLC had no significant impact on the weight loss of PLA. Surface morphologies of PLA and biocomposites showed that PLA exhibited surface erosion; however, the addition of MFLC and Ac-MFLC changed its biodegradation behaviours. Channel formations were observed on the MFLC-0.5 biocomposites. Higher microfibril containing biocomposites showed porous formations, which led to the loosening of the microfibril-PLA interface. The viscoelastic properties of PLA and biocomposites changed considerably after soil burial. *E'* of PLA and all biocomposites decreased; however, *E'* of MFLC/biocomposites decreased more than that of Ac-MFLC, which is attributed to the limited damage between Ac-MFLC–PLA interface during soil burial. Further, annealing effect was observed from the viscoelastic properties of PLA and all biocomposites in the glass transition region as the result of incubation of soil burial which led to a significant decrease in tan δ. No antimicrobial activity was observed against Gram-negative and Gram-positive bacteria, confirming the biotic degradability of biocomposites. The results showed that the presence of both types of MFLC in biocomposites has a significant impact on their viscoelastic properties after biodegradation. The untreated MFLC shows a larger change than the Ac-MFLC. Furthermore, the biodegradation rate of PLA was increased by the presence of MFLC, but was not significantly influenced by the Ac-MFLC. The findings reveal that the addition of Ac-MFLC can be used for the fabrication of PLA biocomposites in industrial applications without affecting the biodegradation properties of polymer matrix.

Supplementary Information The online version contains supplementary material available at https://doi.org/10.1007/s10924-022-02583-2.

Acknowledgements We would like to thank the valuable supports of Ully Kritzler and Zhabiz Vilkiji for soil burial testing, and Enes Aslan for the antimicrobial testing of biocomposites. We also acknowledge the scholarship provided by Republic of Turkey – Ministry of National Education, and Turkish Forestry Service.

Author Contributions **Ferhat Yetiş**: Conceptualization, Methodology, Formal analysis, Investigation, Data curation, Writing – original draft. **Xuqing Liu**: Methodology, Validation, Writing - review & editing, Supervision. **William W. Sampson**: Validation, Writing-review & editing, Supervision. **R. Hugh Gong**: Writing-review & editing, Supervision.

Funding The authors declare that no funds, grants, or other support were received during the preparation of this manuscript.

Declarations

Conflict of Interest The authors declare that they have no known competing financial interests or personal relationships that could have appeared to influence the work reported in this paper.

References

1. Blettler MCM, Garello N, Ginon L, Abrial E, Espinola LA, Wantzen KM (2019) Massive plastic pollution in a mega-river of a developing country: Sediment deposition and ingestion by fish (Prochilodus lineatus), Environ. Pollut 255:113348. https://doi.org/10.1016/j.envpol.2019.113348
2. Chae Y, An YJ (2018) Current research trends on plastic pollution and ecological impacts on the soil ecosystem: A review. Environ Pollut 240:387–395. https://doi.org/10.1016/j.envpol.2018.05.008
3. Anugwom I, Lahtela V, Kallioinen M, Kärki T (2019) Lignin as a functional additive in a biocomposite: Influence on mechanical properties of polylactic acid composites. Ind Crops Prod 140:111704. https://doi.org/10.1016/j.indcrop.2019.111704
4. Gandolfi MG, Zamparini F, Degli Esposti M, Chiellini F, Aparicio C, Fava F, Fabbri P, Taddei P, Prati C (2018) Polylactic acid-based porous scaffolds doped with calcium silicate and dicalcium phosphate dihydrate designed for biomedical application. Mater Sci Eng C 82:163–181. https://doi.org/10.1016/j.msec.2017.08.040
5. Yang S, Bai S, Wang Q (2018) Sustainable packaging biocomposites from polylactic acid and wheat straw: Enhanced

physical performance by solid state shear milling process. Compos Sci Technol 158:34–42. https://doi.org/10.1016/j.compscitech.2017.12.026
6. Liu Q, Yang Q, Zhou Y, Zhao M, Shen Y, Zhou F, Gong RH, Deng B (2018) A facile method of preparing highly porous polylactide microfibers. J Appl Polym Sci 135:45860. https://doi.org/10.1002/app.45860
7. Wang YY, Yu HY, Yang L, Abdalkarim SYH, Chen WL (2019) Enhancing long-term biodegradability and UV-shielding performances of transparent polylactic acid nanocomposite films by adding cellulose nanocrystal-zinc oxide hybrids. Int J Biol Macromol 141:893–905. https://doi.org/10.1016/j.ijbiomac.2019.09.062
8. Meriçer Ç, Minelli M, Giacinti Baschetti M, Lindström T (2017) Water sorption in microfibrillated cellulose (MFC): The effect of temperature and pretreatment. Carbohydr Polym 174:1201–1212. https://doi.org/10.1016/j.carbpol.2017.07.023
9. Castro DO, Karim Z, Medina L, Häggström JO, Carosio F, Svedberg A, Wågberg L, Söderberg D, Berglund LA (2018) The use of a pilot-scale continuous paper process for fire retardant cellulose-kaolinite nanocomposites. Compos Sci Technol 162:215–224. https://doi.org/10.1016/j.compscitech.2018.04.032
10. Oksman K, Aitomäki Y, Mathew AP, Siqueira G, Zhou Q, Butylina S, Tanpichai S, Zhou X, Hooshmand S (2016) Review of the recent developments in cellulose nanocomposite processing. Compos Part A Appl Sci Manuf 83:2–18. https://doi.org/10.1016/j.compositesa.2015.10.041
11. Rojo E, Peresin MS, Sampson WW, Hoeger IC, Vartiainen J, Laine J, Rojas OJ (2015) Comprehensive elucidation of the effect of residual lignin on the physical, barrier, mechanical and surface properties of nanocellulose films. Green Chem. https://doi.org/10.1039/c4gc02398f
12. Ämmälä A, Laitinen O, Sirviö JA, Liimatainen H (2019) Key role of mild sulfonation of pine sawdust in the production of lignin containing microfibrillated cellulose by ultrafine wet grinding. Ind Crops Prod 140:111664. https://doi.org/10.1016/j.indcrop.2019.111664
13. Chen Y, Fan D, Han Y, Lyu S, Lu Y, Li G, Jiang F, Wang S (2018) Effect of high residual lignin on the properties of cellulose nanofibrils/films. Cellulose 25:6421–6431. https://doi.org/10.1007/s10570-018-2006-x
14. Yousefi H, Azari V, Khazaeian A (2018) Direct mechanical production of wood nanofibers from raw wood microparticles with no chemical treatment. Ind Crops Prod 115:26–31. https://doi.org/10.1016/j.indcrop.2018.02.020
15. Visanko M, Sirviö JA, Piltonen P, Sliz R, Liimatainen H, Illikainen M (2017) Mechanical fabrication of high-strength and redispersible wood nanofibers from unbleached groundwood pulp. Cellulose 24:4173–4187. https://doi.org/10.1007/s10570-017-1406-7
16. Tripathi A, Ferrer A, Khan SA, Rojas OJ (2017) Morphological and Thermochemical Changes upon Autohydrolysis and Microemulsion Treatments of Coir and Empty Fruit Bunch Residual Biomass to Isolate Lignin-Rich Micro- and Nanofibrillar Cellulose, ACS Sustain. Chem Eng. https://doi.org/10.1021/acssuschemeng.6b02838
17. Jiang Y, Liu X, Yang Q, Song X, Qin C, Wang S, Li K (2019) Effects of residual lignin on composition, structure and properties of mechanically defibrillated cellulose fibrils and films. Cellulose 26:1577–1593. https://doi.org/10.1007/s10570-018-02229-4
18. Lu H, Zhang L, Liu C, He Z, Zhou X, Ni Y (2018) A novel method to prepare lignocellulose nanofibrils directly from bamboo chips. Cellulose 25:7043–7051. https://doi.org/10.1007/s10570-018-2067-x
19. Oliaei E, Lindén PA, Wu Q, Berthold F, Berglund L, Lindström T (2019) Microfibrillated lignocellulose (MFLC) and nanopaper films from unbleached kraft softwood pulp, Cellulose.1–17. https://doi.org/10.1007/s10570-019-02934-8
20. Herrera M, Thitiwutthisakul K, Yang X, on Rujitanaroj P, Rojas R, Berglund L (2018) Preparation and evaluation of high-lignin content cellulose nanofibrils from eucalyptus pulp, Cellulose. https://doi.org/10.1007/s10570-018-1764-9
21. Osong SH, Norgren S, Engstrand P (2013) An approach to produce nano-ligno-cellulose from mechanical pulp fine materials. Nord Pulp Pap Res J 28:472–479. https://doi.org/10.3183/npprj-2013-28-04-p472-479
22. Abe K, Nakatsubo F, Yano H (2009) High-strength nanocomposite based on fibrillated chemi-thermomechanical pulp. Compos Sci Technol 69:2434–2437. https://doi.org/10.1016/j.compscitech.2009.06.015
23. Yetiş F, Liu X, Sampson WW, Gong RH (2020) Acetylation of lignin containing microfibrillated cellulose and its reinforcing effect for polylactic acid. Eur Polym J. https://doi.org/10.1016/j.eurpolymj.2020.109803
24. Karamanlioglu M, Robson GD (2013) The influence of biotic and abiotic factors on the rate of degradation of poly(lactic) acid (PLA) coupons buried in compost and soil. Polym Degrad Stab 98:2063–2071. https://doi.org/10.1016/j.polymdegradstab.2013.07.004
25. Fortunati E, Luzi F, Puglia D, Dominici F, Santulli C, Kenny JM, Torre L (2014) Investigation of thermo-mechanical, chemical and degradative properties of PLA-limonene films reinforced with cellulose nanocrystals extracted from Phormium tenax leaves. Eur Polym J 56:77–91. https://doi.org/10.1016/j.eurpolymj.2014.03.030
26. Jin X, Yu X, Yang C, dong Qi X, zhou Lei Y, Wang Y (2019) Crystallization and hydrolytic degradation behaviors of poly(L-lactide) induced by carbon nanofibers with different surface modifications. Polym Degrad Stab 170:109014. https://doi.org/10.1016/j.polymdegradstab.2019.109014
27. Phua YJ, Lau NS, Sudesh K, Chow WS, Mohd Ishak ZA (2012) Biodegradability studies of poly(butylene succinate)/organo-montmorillonite nanocomposites under controlled compost soil conditions: Effects of clay loading and compatibiliser. Polym Degrad Stab 97:1345–1354. https://doi.org/10.1016/j.polymdegradstab.2012.05.024
28. Aslan E, Vyas C, Mieles JY, Humphreys G, Diver C, Bartolo P (2022) Preliminary characterization of a polycaprolactone-surgihoneyRO electrospun mesh for skin tissue engineering. Mater (Basel) 15:89. https://doi.org/10.3390/MA15010089/S1
29. Fukushima K, Tabuani D, Abbate C, Arena M, Ferreri L (2010) Effect of sepiolite on the biodegradation of poly(lactic acid) and polycaprolactone. Polym Degrad Stab 95:2049–2056. https://doi.org/10.1016/j.polymdegradstab.2010.07.004
30. Bitinis N, Fortunati E, Verdejo R, Bras J, Kenny JM, Torre L, López-Manchado MA (2013) Poly(lactic acid)/natural rubber/cellulose nanocrystal bionanocomposites. Part II: Properties evaluation. Carbohydr Polym 96:621–627. https://doi.org/10.1016/j.carbpol.2013.03.091
31. Luzi F, Fortunati E, Puglia D, Petrucci R, Kenny JM, Torre L (2015) Study of disintegrability in compost and enzymatic degradation of PLA and PLA nanocomposites reinforced with cellulose nanocrystals extracted from Posidonia Oceanica. Polym Degrad Stab 121:105–115. https://doi.org/10.1016/j.polymdegradstab.2015.08.016
32. Karamanlioglu M, Preziosi R, Robson GD (2017) Abiotic and biotic environmental degradation of the bioplastic polymer poly(lactic acid): A review. Polym Degrad Stab 137:122–130. https://doi.org/10.1016/j.polymdegradstab.2017.01.009
33. Iglesias-Montes ML, Luzi F, Dominici F, Torre L, Manfredi LB, Cyras VP, Puglia D (2021) Migration and Degradation in Composting Environment of Active Polylactic Acid Bilayer Nanocomposites Films: Combined Role of Umbelliferone, Lignin and Cellulose Nanostructures, Polym. Vol. 13, Page 282. 13 (2021) 282. https://doi.org/10.3390/POLYM13020282

34. Lu H, Madbouly SA, Schrader JA, Srinivasan G, Mccabe KG, Grewell D, Kessler MR, Graves WR (2014) Biodegradation behavior of poly(lactic acid) (PLA)/Distiller's dried grains with solubles (DDGS) composites, ACS Sustain. Chem Eng 2:2699–2706. https://doi.org/10.1021/sc500440q
35. Lv S, Zhang Y, Gu J, Tan H (2017) Biodegradation behavior and modelling of soil burial effect on degradation rate of PLA blended with starch and wood flour. Colloids Surf B Biointerfaces 159:800–808. https://doi.org/10.1016/j.colsurfb.2017.08.056
36. da Silva TF, Menezes F, Montagna LS, Lemes AP, Passador FR (2019) Effect of lignin as accelerator of the biodegradation process of poly(lactic acid)/lignin composites. Mater Sci Eng B Solid-State Mater Adv Technol 251:114441. https://doi.org/10.1016/j.mseb.2019.114441
37. Laycock B, Nikolić M, Colwell JM, Gauthier E, Halley P, Bottle S, George G (2017) Lifetime prediction of biodegradable polymers. Prog Polym Sci 71:144–189. https://doi.org/10.1016/j.progpolymsci.2017.02.004
38. Scaffaro R, Maio A, Gulino EF, Pitarresi G (2020) Lignocellulosic fillers and graphene nanoplatelets as hybrid reinforcement for polylactic acid: Effect on mechanical properties and degradability. Compos Sci Technol 190:108008. https://doi.org/10.1016/j.compscitech.2020.108008
39. Chan CM, Vandi LJ, Pratt S, Halley P, Richardson D, Werker A, Laycock B (2019) Insights into the biodegradation of PHA / wood composites: Micro- and macroscopic changes. Sustain Mater Technol 21:e00099. https://doi.org/10.1016/j.susmat.2019.e00099
40. feng Zuo Y, Gu J, Qiao Z, Tan H, Cao J, Zhang Y (2015) Effects of dry method esterification of starch on the degradation characteristics of starch/polylactic acid composites. Int J Biol Macromol 72:391–402. https://doi.org/10.1016/j.ijbiomac.2014.08.038
41. Zhang Q, Lei H, Cai H, Han X, Lin X, Qian M, Zhao Y, Huo E, Villota EM, Mateo W (2020) Improvement on the properties of microcrystalline cellulose/polylactic acid composites by using activated biochar. J Clean Prod 252:119898. https://doi.org/10.1016/j.jclepro.2019.119898
42. Shojaeiarani J, Bajwa DS, Stark NM, Bajwa SG (2019) Rheological properties of cellulose nanocrystals engineered polylactic acid nanocomposites. Compos Part B Eng. https://doi.org/10.1016/j.compositesb.2018.12.128
43. Nakagaito AN, Fujimura A, Sakai T, Hama Y, Yano H (2009) Production of microfibrillated cellulose (MFC)-reinforced polylactic acid (PLA) nanocomposites from sheets obtained by a papermaking-like process. Compos Sci Technol 69:1293–1297. https://doi.org/10.1016/j.compscitech.2009.03.004
44. Larsson K, Berglund LA, Ankerfors M, Lindström T (2012) Polylactide latex/nanofibrillated cellulose bionanocomposites of high nanofibrillated cellulose content and nanopaper network structure prepared by a papermaking route. J Appl Polym Sci. https://doi.org/10.1002/app.36413
45. Zhang Y, Wu J, Wang B, Sui X, Zhong Y, Zhang L, Mao Z, Xu H (2017) Cellulose nanofibril-reinforced biodegradable polymer composites obtained via a Pickering emulsion approach. Cellulose 24:3313–3322. https://doi.org/10.1007/s10570-017-1324-8
46. Spinella S, Lo Re G, Liu B, Dorgan J, Habibi Y, Leclère P, Raquez JM, Dubois P, Gross RA (2015) Polylactide/cellulose nanocrystal nanocomposites: Efficient routes for nanofiber modification and effects of nanofiber chemistry on PLA reinforcement. Polym (Guildf). https://doi.org/10.1016/j.polymer.2015.02.048
47. Zhou L, He H, Li M, Huang S, Mei C, Wu Q (2018) Enhancing mechanical properties of poly(lactic acid) through its in-situ crosslinking with maleic anhydride-modified cellulose nanocrystals from cottonseed hulls. Ind Crops Prod 112:449–459. https://doi.org/10.1016/j.indcrop.2017.12.044
48. Fortunati E, Peltzer M, Armentano I, Torre L, Jiménez A, Kenny JM (2012) Effects of modified cellulose nanocrystals on the barrier and migration properties of PLA nano-biocomposites. Carbohydr Polym. https://doi.org/10.1016/j.carbpol.2012.06.025
49. Pérez-Fonseca AA, Robledo-Ortíz JR, González-Núñez R, Rodrigue D (2016) Effect of thermal annealing on the mechanical and thermal properties of polylactic acid-cellulosic fiber biocomposites. J Appl Polym Sci 133. https://doi.org/10.1002/app.43750
50. Orue A, Eceiza A, Arbelaiz A (2018) The effect of sisal fiber surface treatments, plasticizer addition and annealing process on the crystallization and the thermo-mechanical properties of poly(lactic acid) composites, Ind. Crops Prod 118:321–333. https://doi.org/10.1016/j.indcrop.2018.03.068
51. Oyama HT, Tanishima D, Ogawa R (2017) Biologically Safe Poly(l-lactic acid) Blends with Tunable Degradation Rate: Microstructure, Degradation Mechanism, and Mechanical Properties. Biomacromolecules 18:1281–1292. https://doi.org/10.1021/acs.biomac.7b00016
52. Yang S, Madbouly SA, Schrader JA, Srinivasan G, Grewell D, McCabe KG, Kessler MR, Graves WR (2015) Characterization and biodegradation behavior of bio-based poly(lactic acid) and soy protein blends for sustainable horticultural applications. Green Chem 17:380–393. https://doi.org/10.1039/c4gc01482k
53. Mosnáčková K, Danko M, Šišková A, Falco LM, Janigová I, Chmela Å, Vanovčanová Z, Omaníková L, Chodák I, Mosnáček J (2017) Complex study of the physical properties of a poly(lactic acid)/poly(3-hydroxybutyrate) blend and its carbon black composite during various outdoor and laboratory ageing conditions. RSC Adv 7:47132–47142. https://doi.org/10.1039/c7ra08869h
54. Mathews SL, Pawlak J, Grunden AM (2015) Bacterial biodegradation and bioconversion of industrial lignocellulosic streams. Appl Microbiol Biotechnol 99:2939–2954. https://doi.org/10.1007/s00253-015-6471-y
55. Wilhelm RC, Singh R, Eltis LD, Mohn WW (2019) Bacterial contributions to delignification and lignocellulose degradation in forest soils with metagenomic and quantitative stable isotope probing. ISME J 13:413–429. https://doi.org/10.1038/s41396-018-0279-6
56. Bi R, Berglund J, Vilaplana F, McKee LS, Henriksson G The degree of acetylation affects the microbial degradability of mannans,Polym. Degrad. Stab.133 (2016)36–46. https://doi.org/10.1016/j.polymdegradstab.2016.07.009